Supplement of

A food crop yield emulator for integration in the compact Earth system model OSCAR (OSCAR-crop v1.0)

Xinrui Liu et al.

Correspondence to: Xinrui Liu (liuxinrui@iiasa.ac.at)

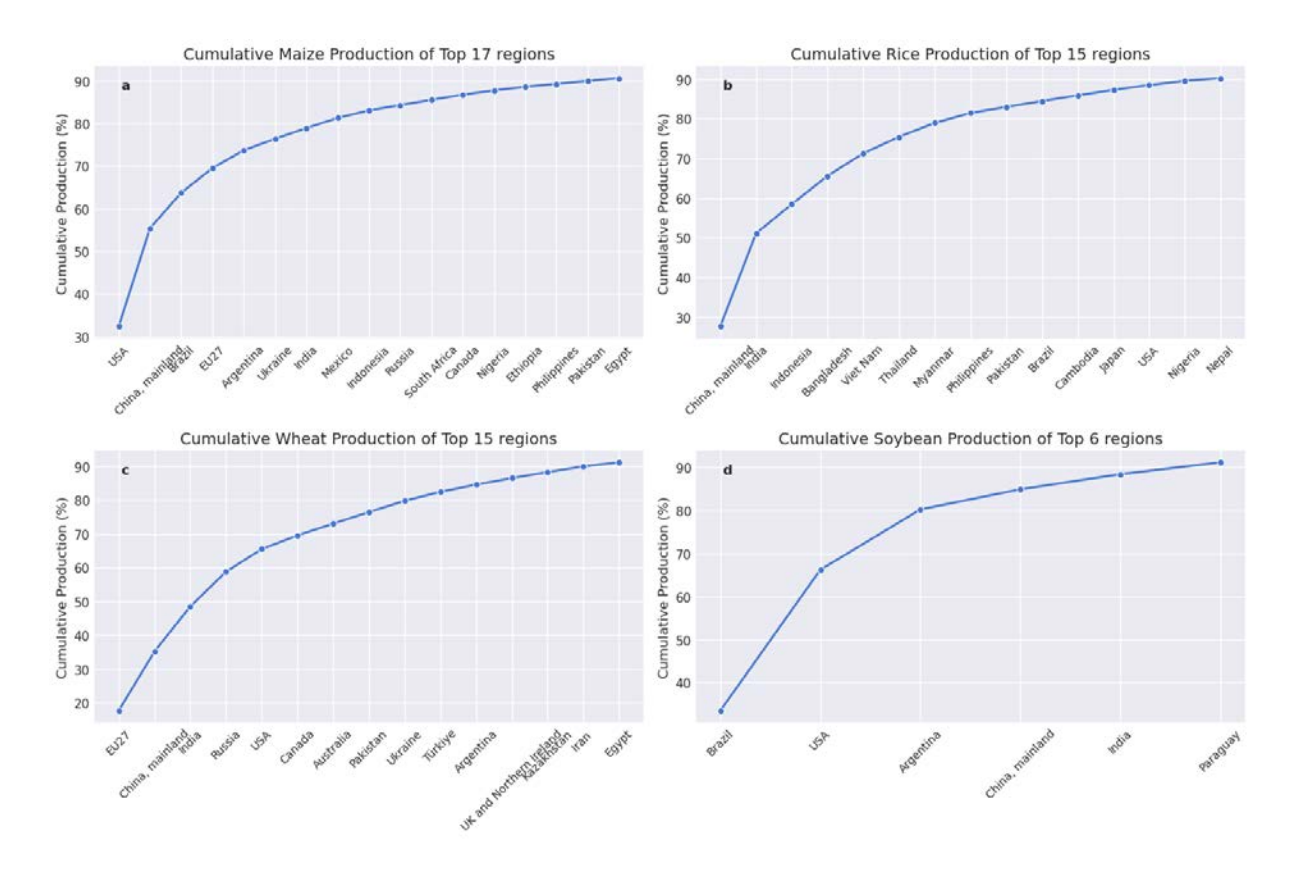


Figure S1. Top producing regions during the period of 2014 to 2023.

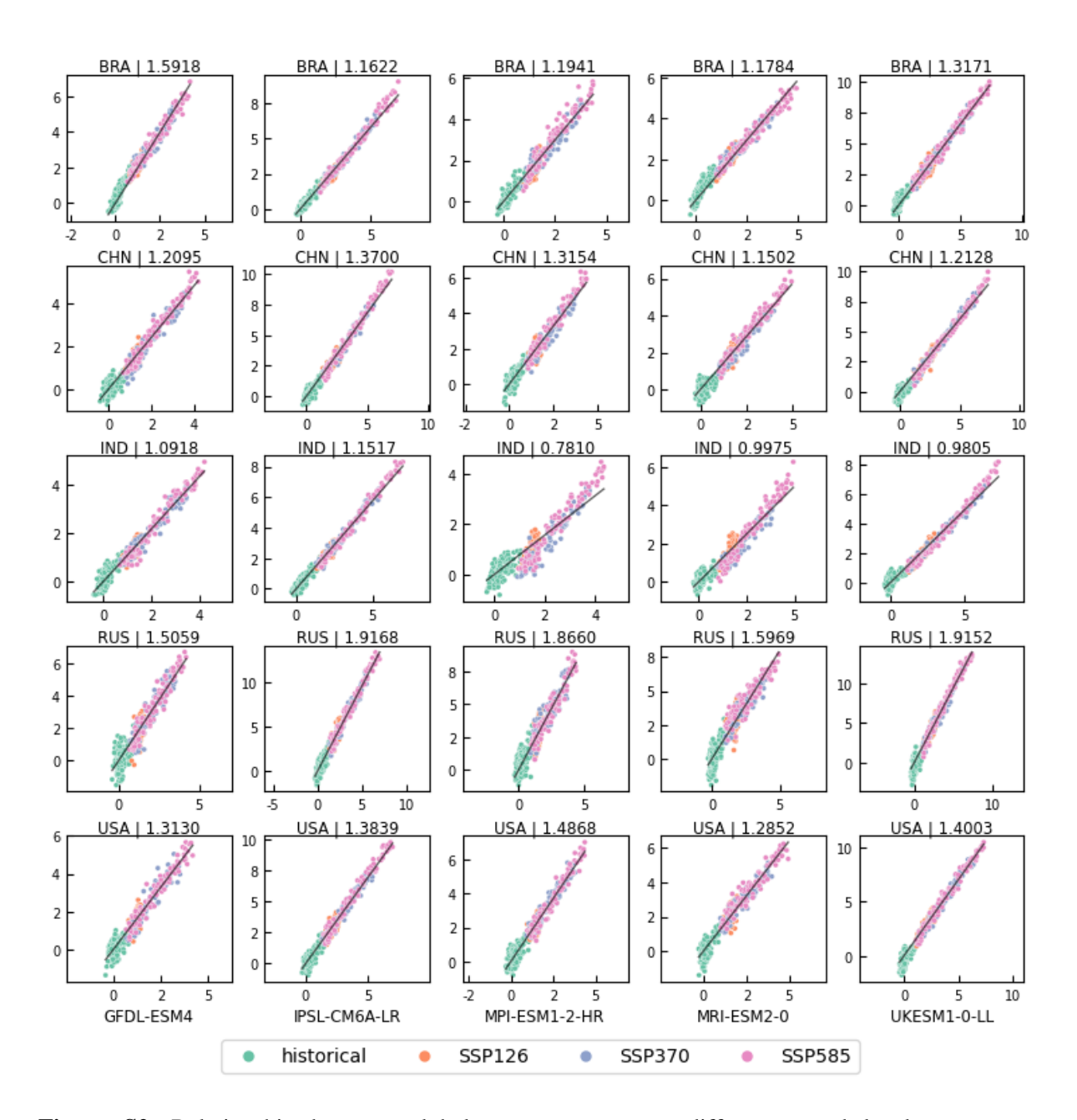


Figure S2. Relationship between global mean temperature differences and local temperature differences using the first concatenation scheme. Subplots in each row and column represent results from different countries (Brazil, mainland China, India, Russia, and the USA) and ESMs (GFDL-ESM4, IPSL-CM6A-LR, MPI-ESM1-2-HR, MRI-ESM2-0 and UKESM1-0-LL). The values next to the regional code represent the linear coefficients.

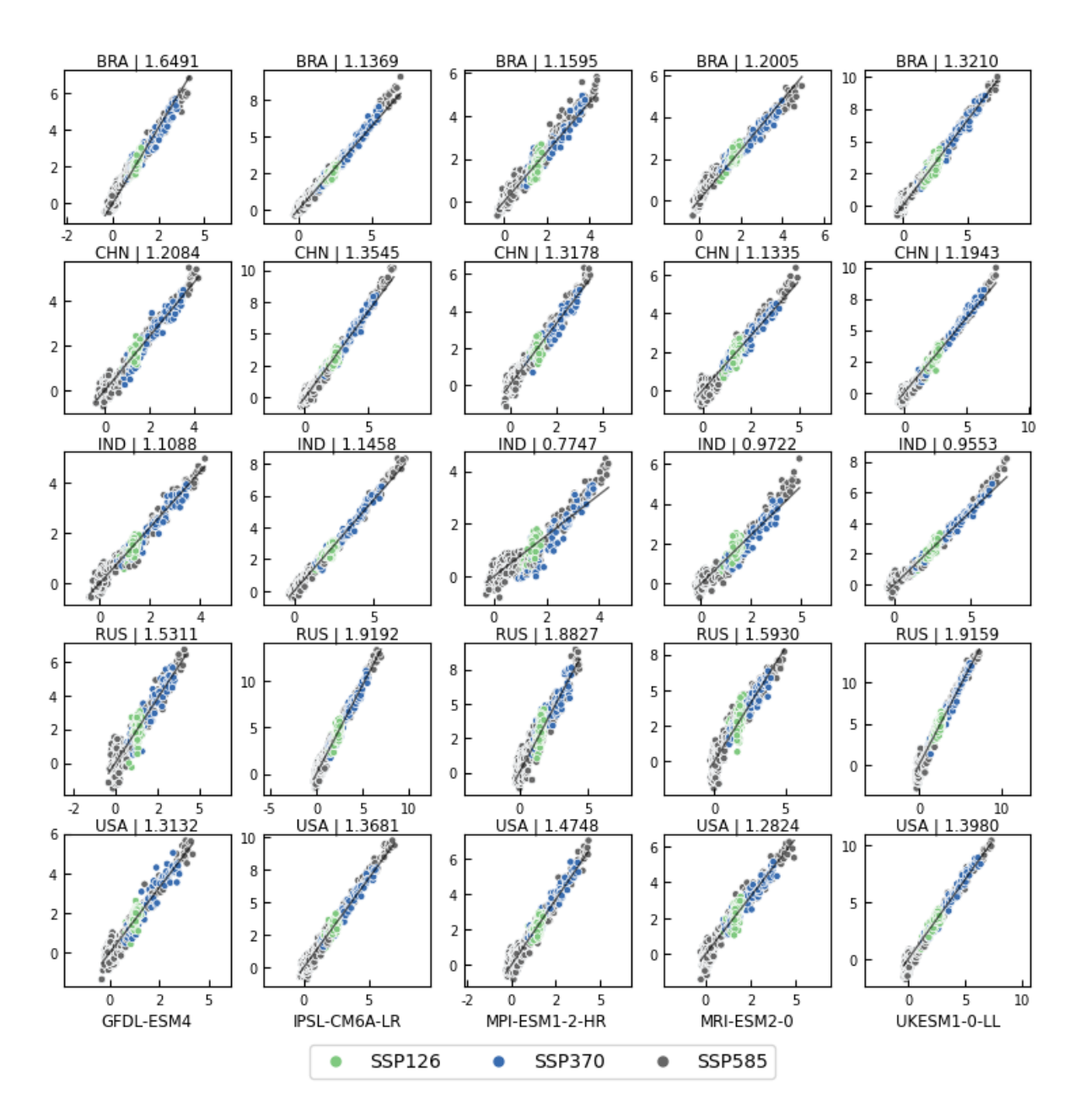


Figure S3. Relationship between global mean temperature differences and local temperature differences using the second concatenation scheme. Subplots in each row and column represent results from different countries (Brazil, mainland China, India, Russia, and the USA) and ESMs (GFDL-ESM4, IPSL-CM6A-LR, MPI-ESM1-2-HR, MRI-ESM2-0 and UKESM1-0-LL), respectively. The values next to the regional code represent the linear coefficients.

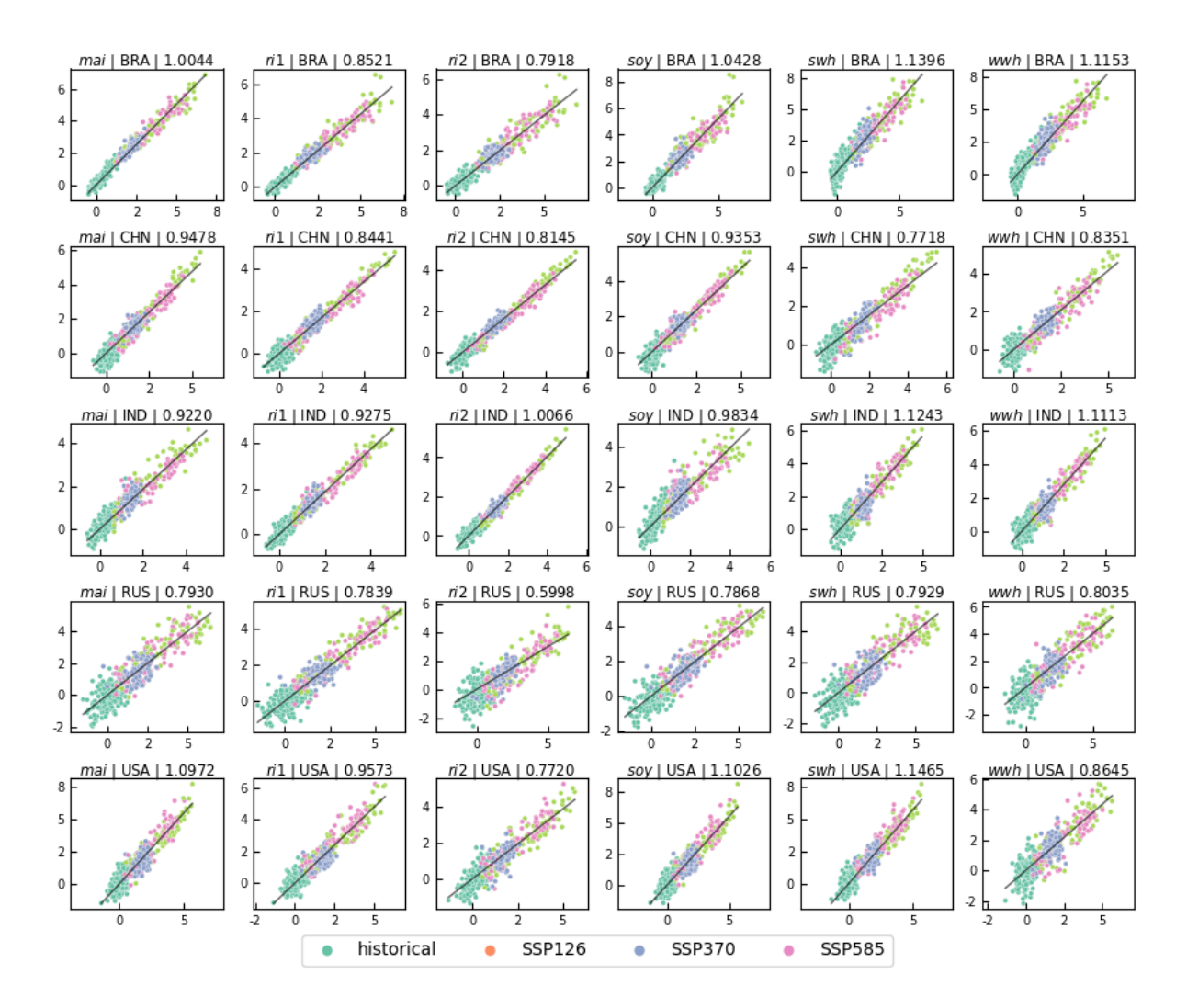


Figure S4. Relationship between local temperature differences and crop-specific growing season temperature differences under rainfed condition using the first concatenation scheme. Subplots in each row and column represent results from different countries (Brazil, mainland China, India, Russia, and the USA) and crop species. The results are from GFDL-ESM4. The values next to the regional code represent the linear coefficients.

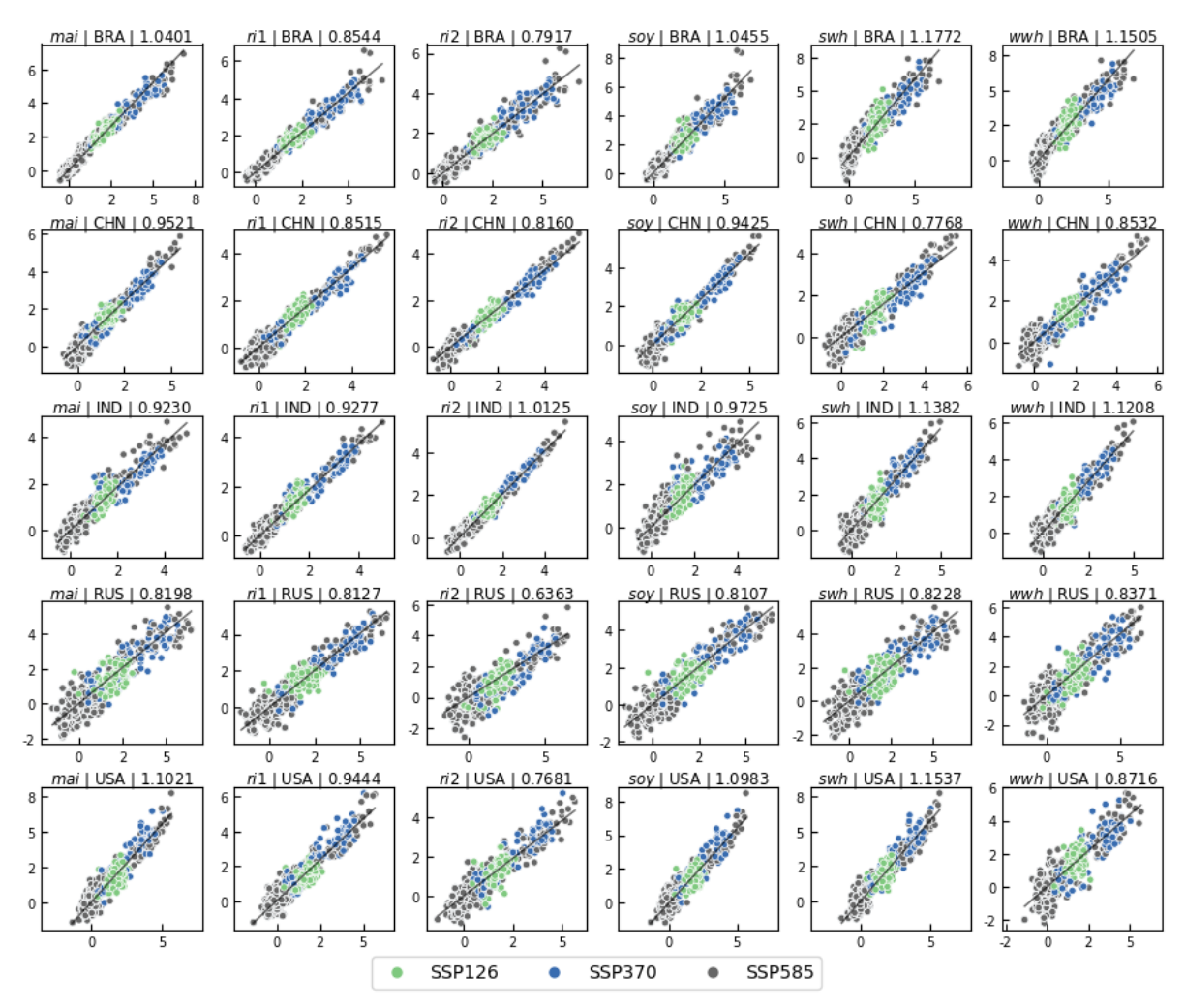


Figure S5. Relationship between local temperature differences and crop-specific growing season temperature differences under rainfed condition using the second concatenation scheme. Subplots in each row and column represent results from different countries (Brazil, mainland China, India, Russia, and the USA) and crop species. The results are from GFDL-ESM4. The values next to the regional code represent the linear coefficients.

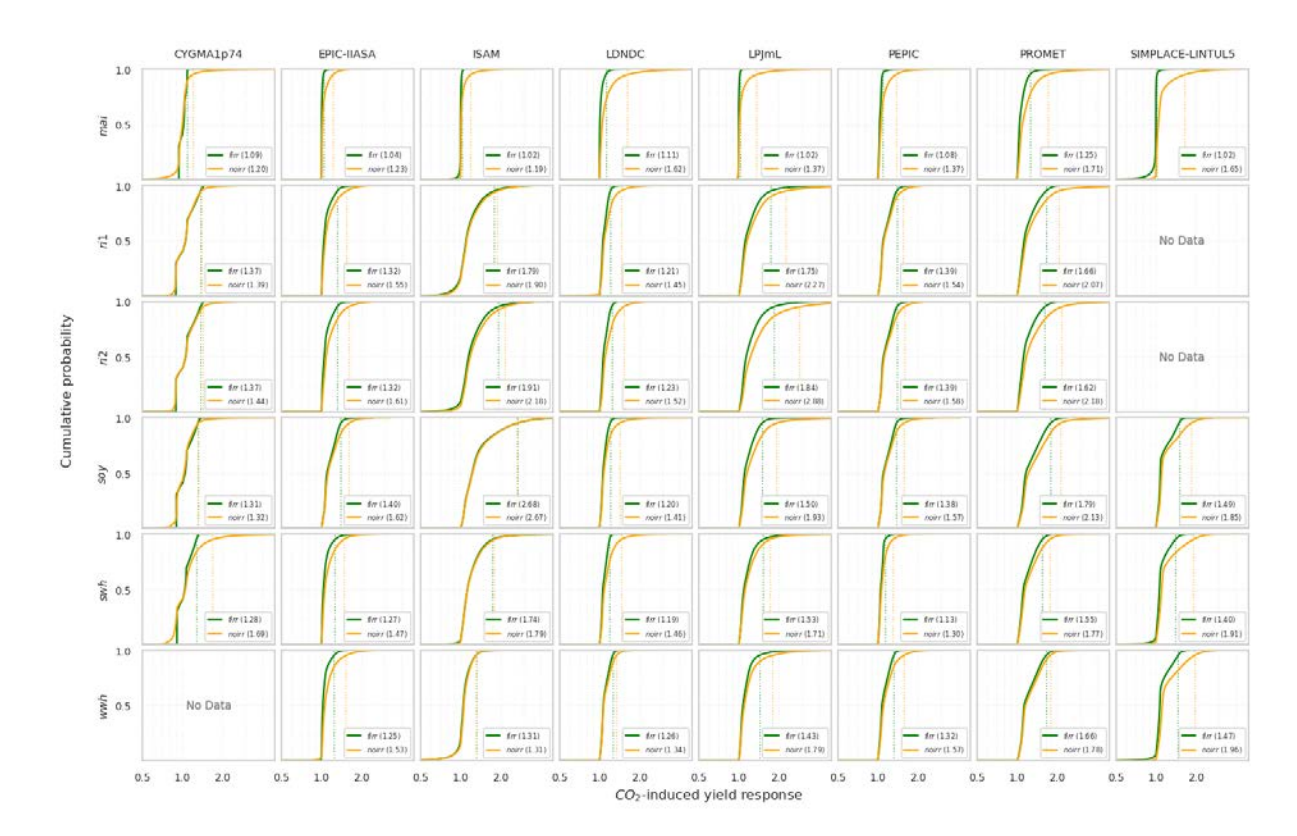


Figure S6. Cumulative probability of regional crop- and model-specific yield responses induced by CO₂. Values in the brackets represent the 95% percentiles of *firr* and *noirr* crops.

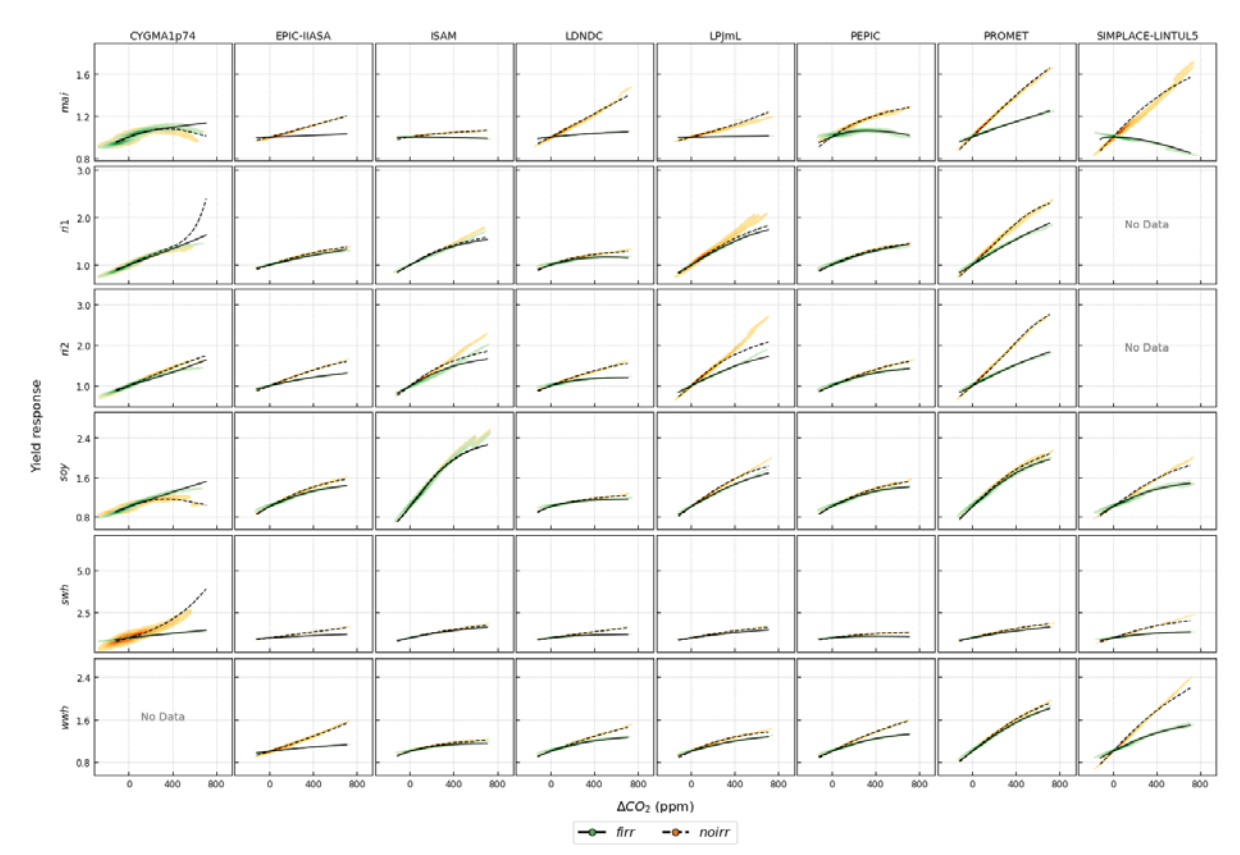


Figure S7. Kernel density estimation of global crop yield responses [CO₂] change (ppm) across eight GGCMs under historical, SSP126, SSP370, and SSP585, including extreme-value regions. Black lines indicate aggregated results from the crop emulator. Black lines indicate aggregated results from the crop emulator. Green shades and orange shades represent *firr* and *noirr* conditions, separately. Darker shades suggest higher density.

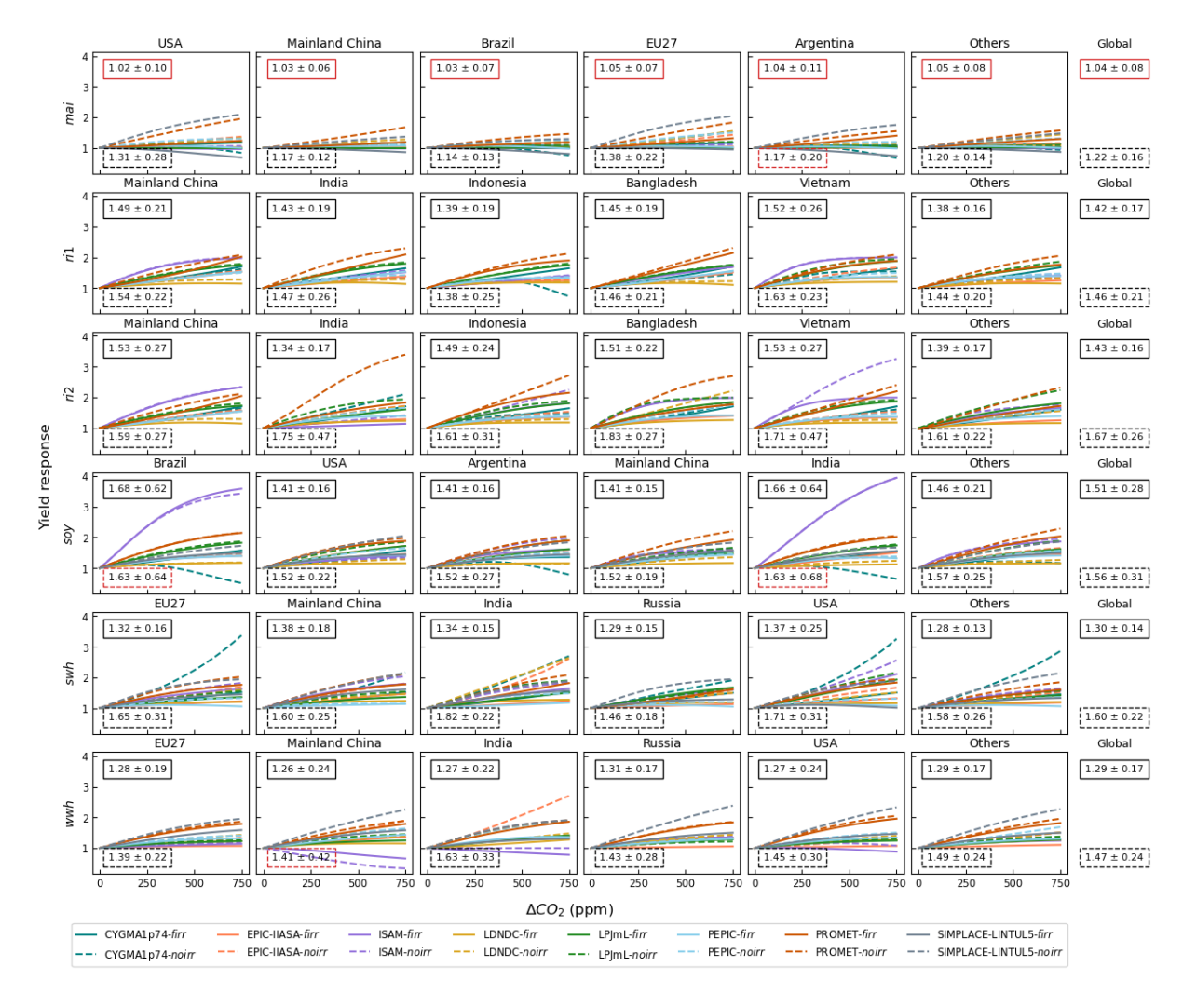


Figure S8. Region- and crop-specific yield responses to [CO₂] change (ppm). Boxes show averages and standard deviations of end-of-century (2069–2099) yield responses for *firr* (solid lines) and *noirr* (dashed lines) crops under SSP585. Red box outlines indicate negative net yield responses.

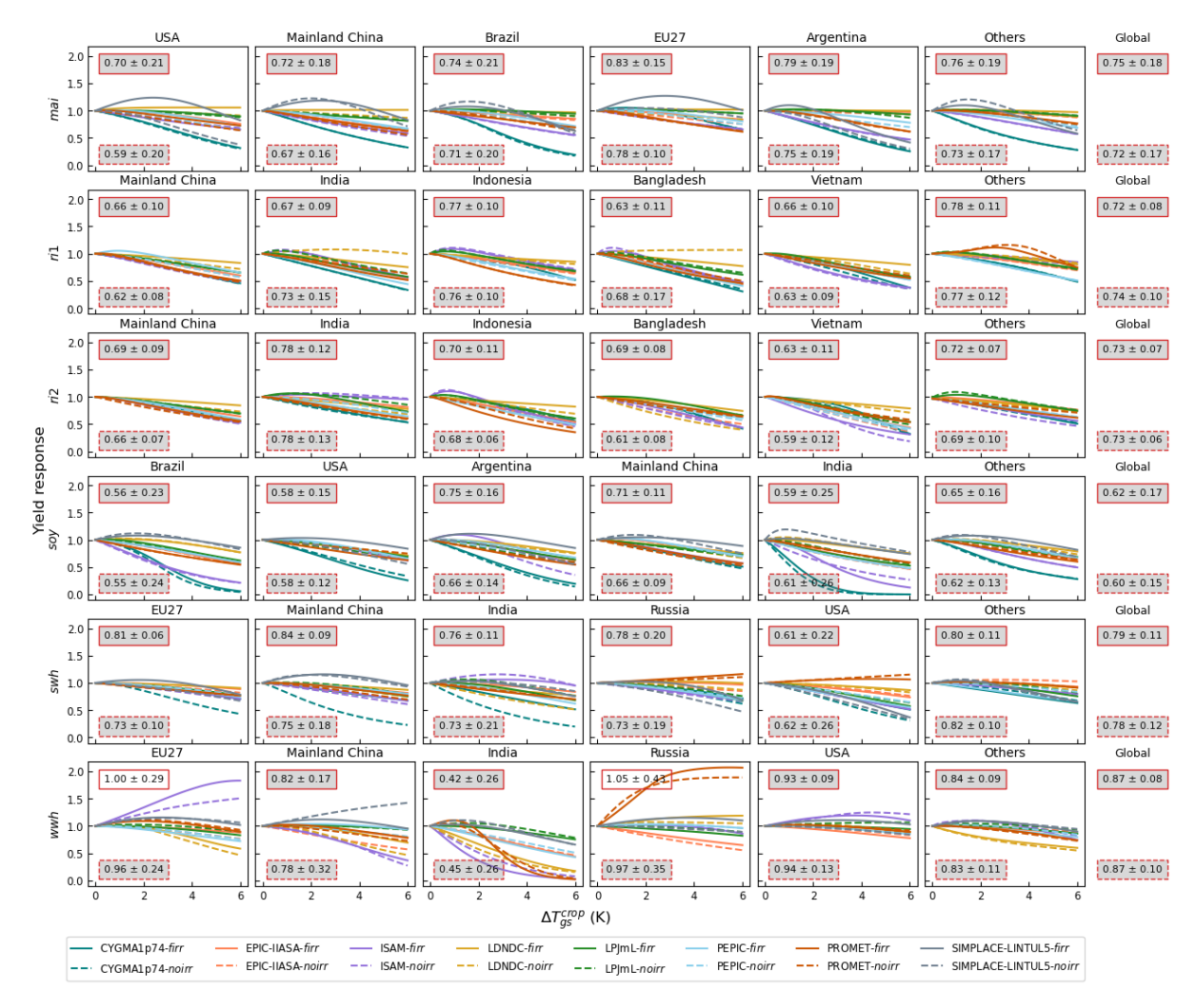


Figure S9. Region- and crop-specific yield responses to growing season temperature change (K). Boxes show averages and standard deviations of end-of-century (2069–2099) yield responses for *firr* (solid lines) and *noirr* (dashed lines) crops under SSP585. Boxes with gray shades indicate end-of-century negative net yield responses. Red box outlines indicate negative net yield responses.

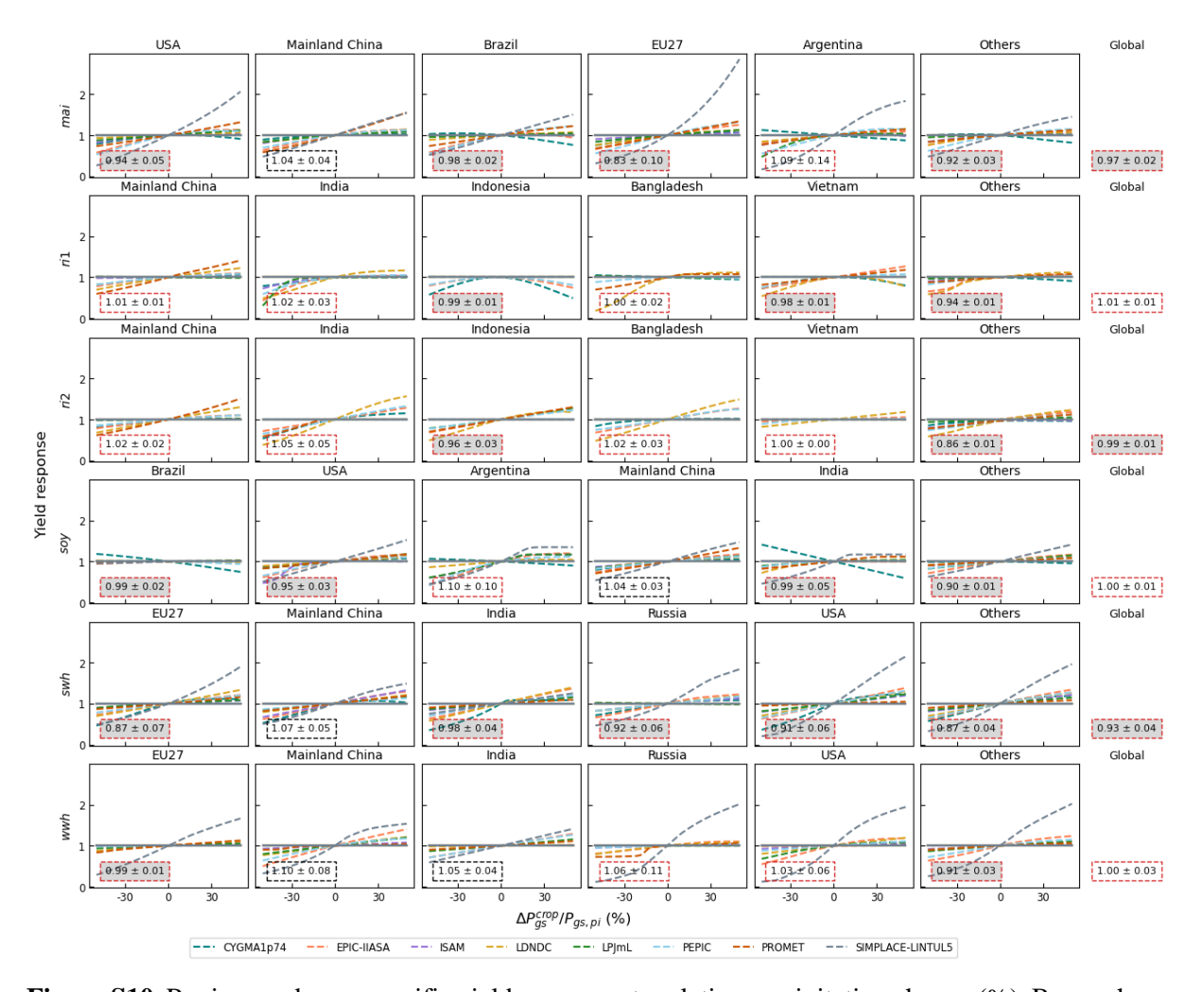


Figure S10. Region- and crop-specific yield responses to relative precipitation change (%). Boxes show averages and standard deviations of end-of-century (2069–2099) yield responses for *noirr* (dashed lines) crops under SSP585. Boxes with gray shades indicate end-of-century negative yield responses. Red box outlines indicate negative net yield responses.

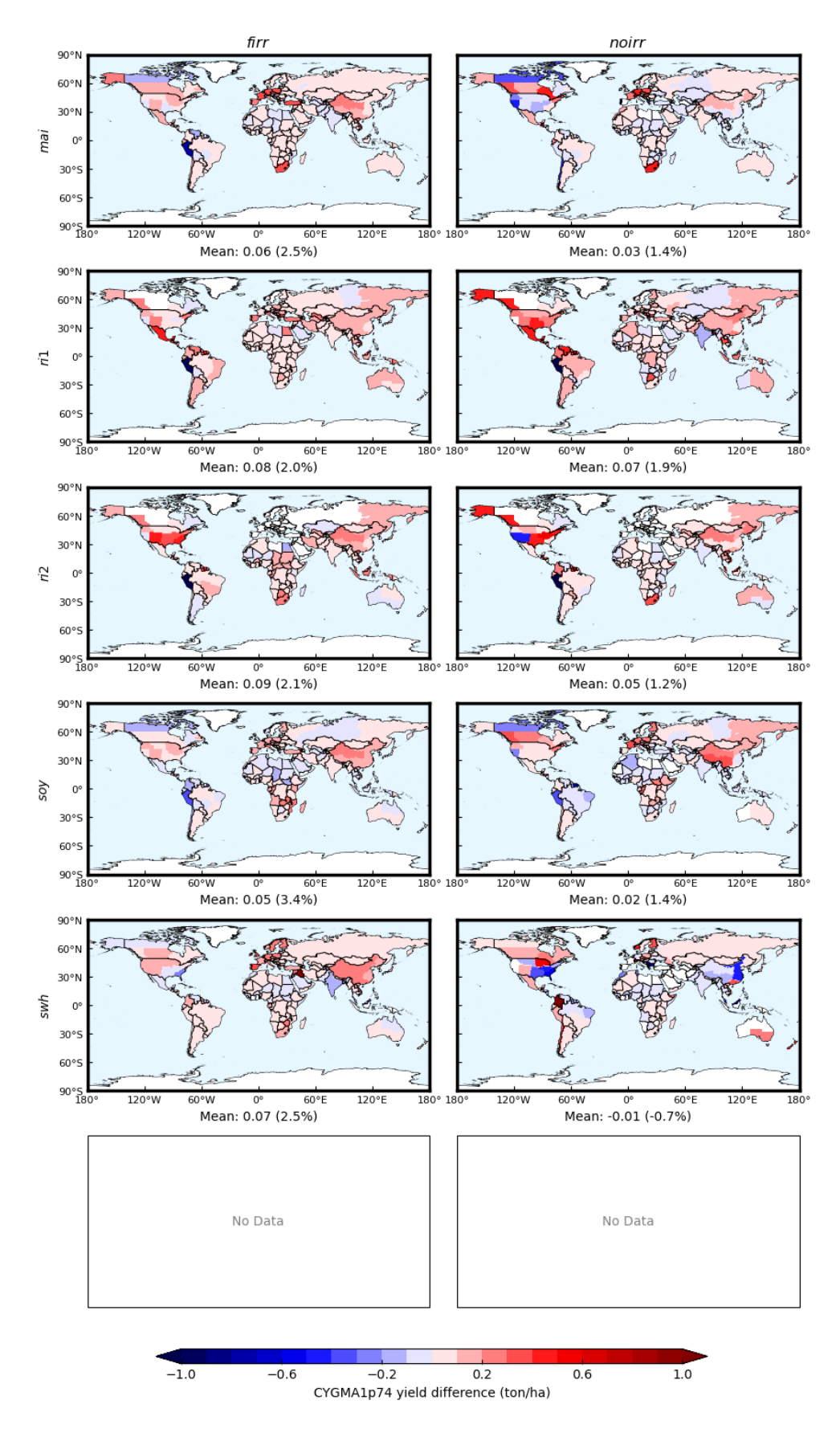


Figure S11. Yield differences between original and CYGMA1p74-based emulated crop yields under SSP585.

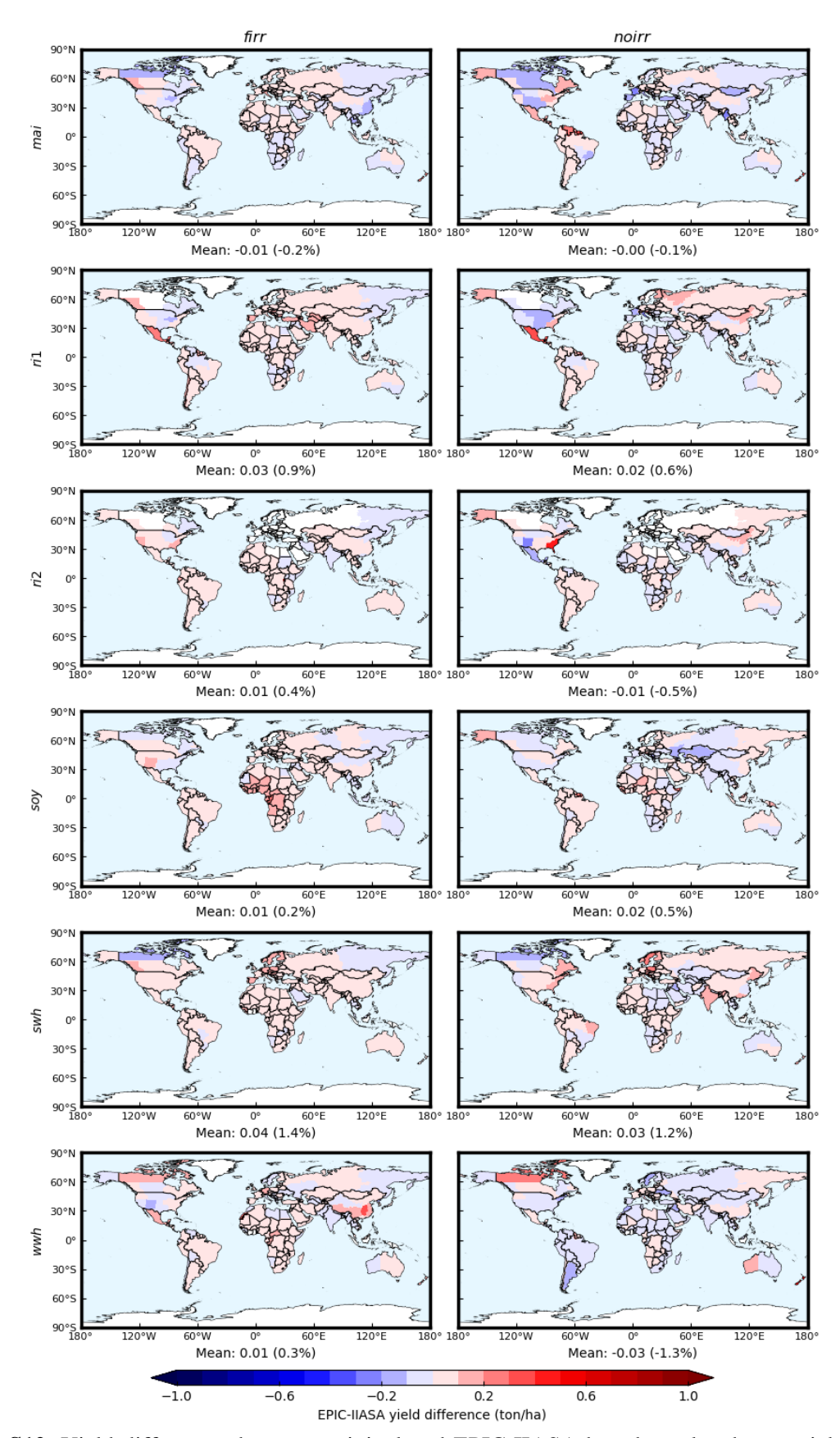


Figure S12. Yield differences between original and EPIC-IIASA-based emulated crop yields under SSP585.

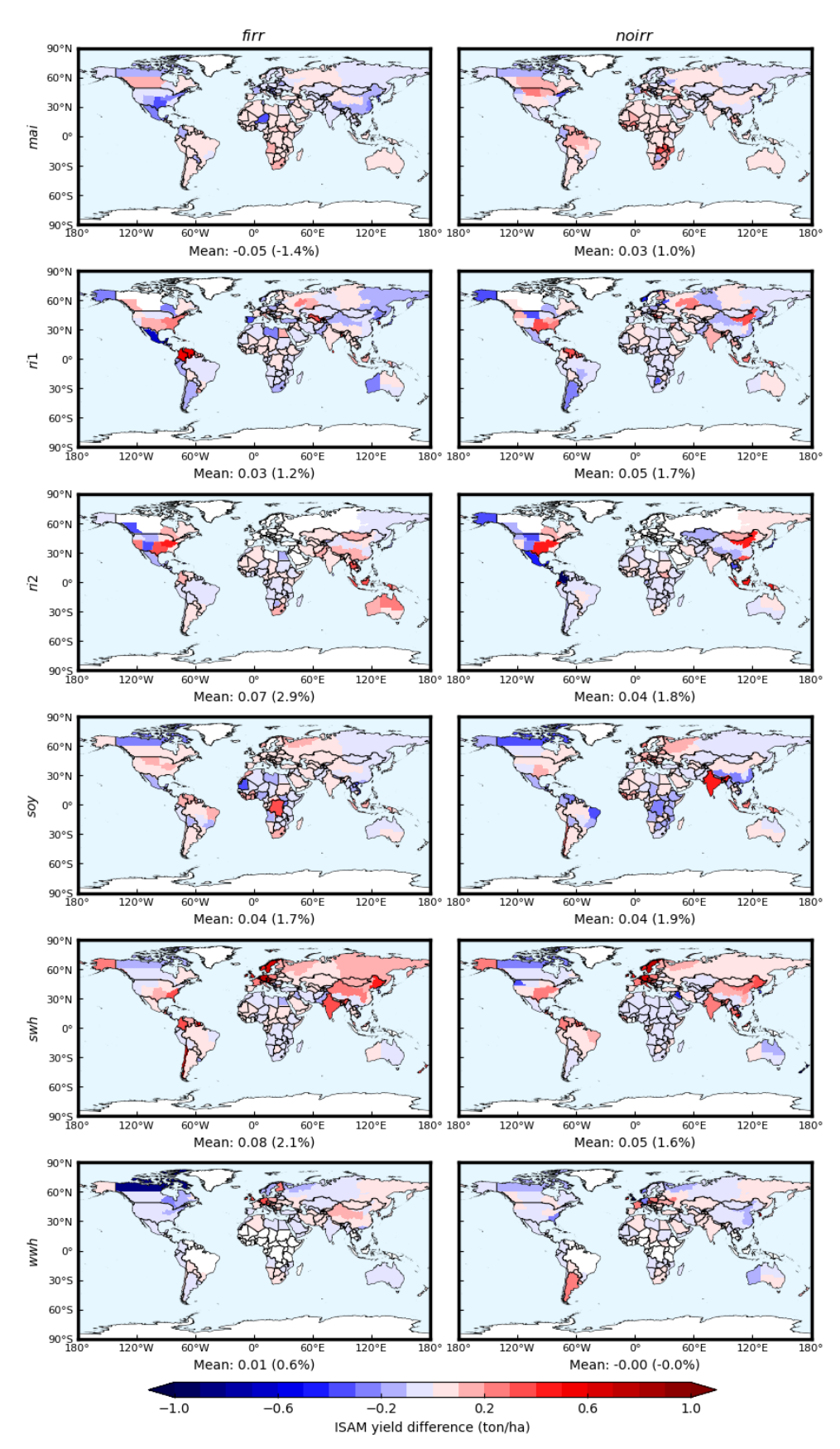


Figure S13. Yield differences between original and ISAM-based emulated crop yields under SSP585.

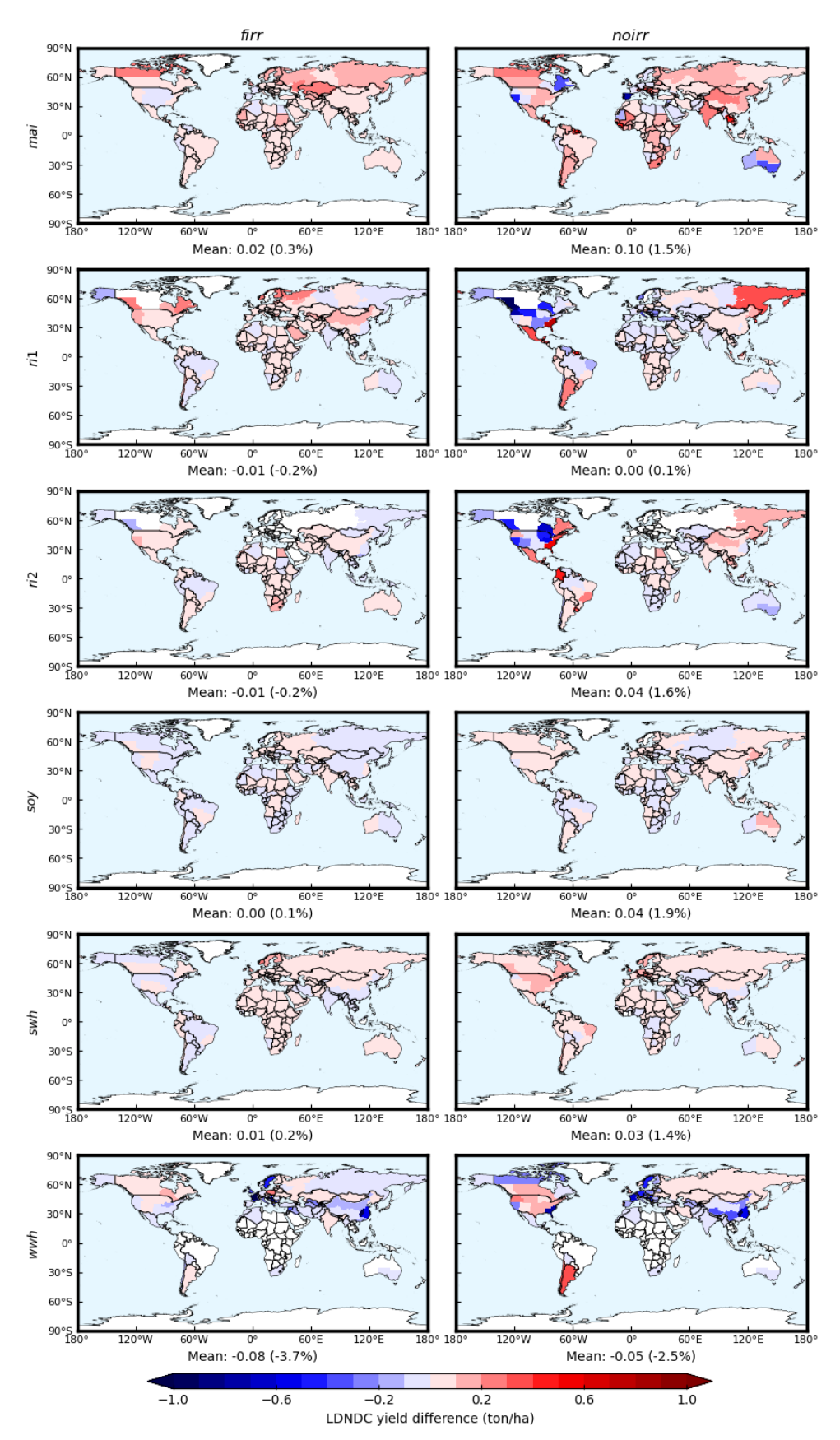


Figure S14. Yield differences between original and LDNDC-based emulated crop yields under SSP585.

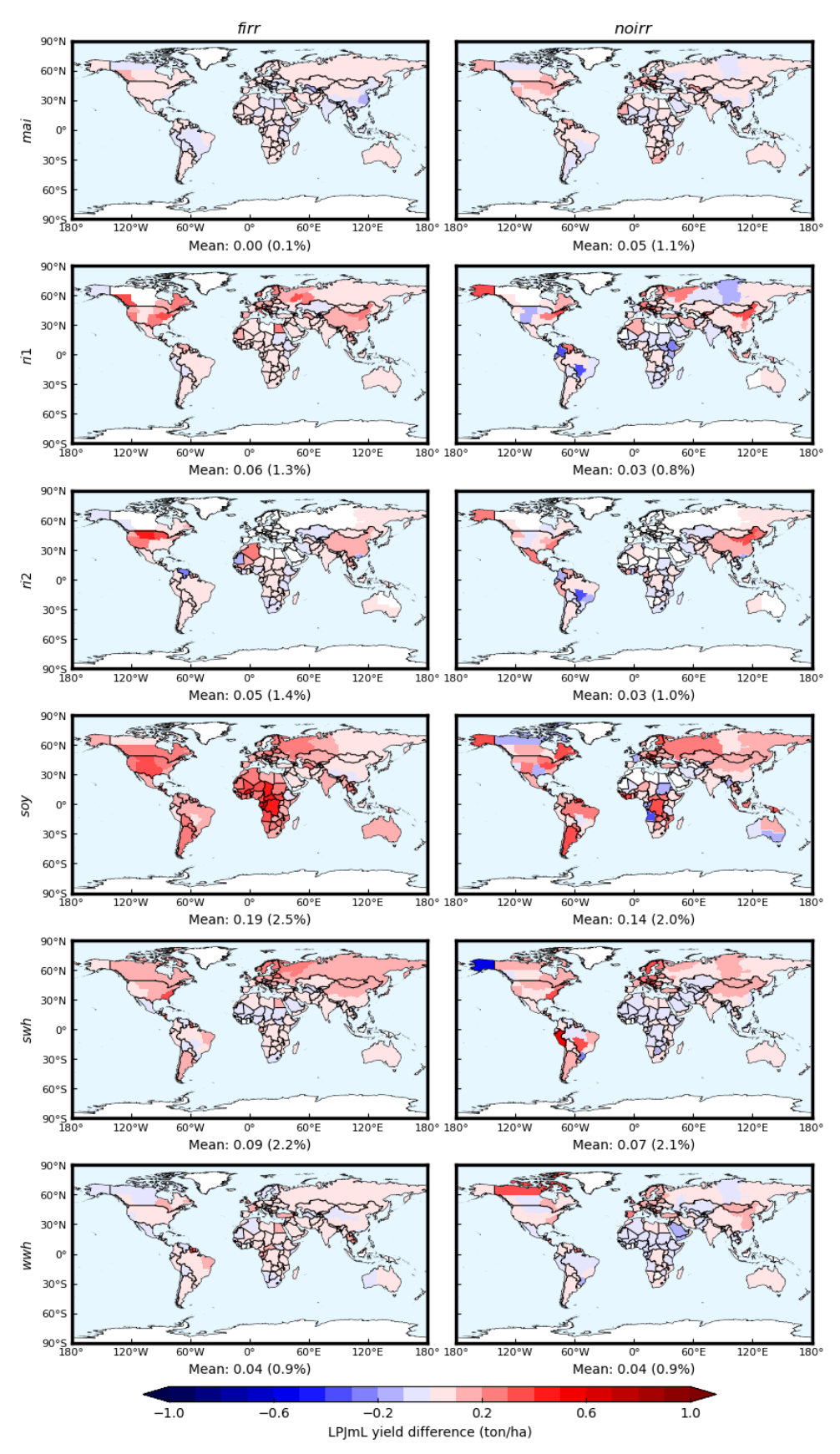


Figure S15. Yield differences between original and LPJmL-based emulated crop yields under SSP585.

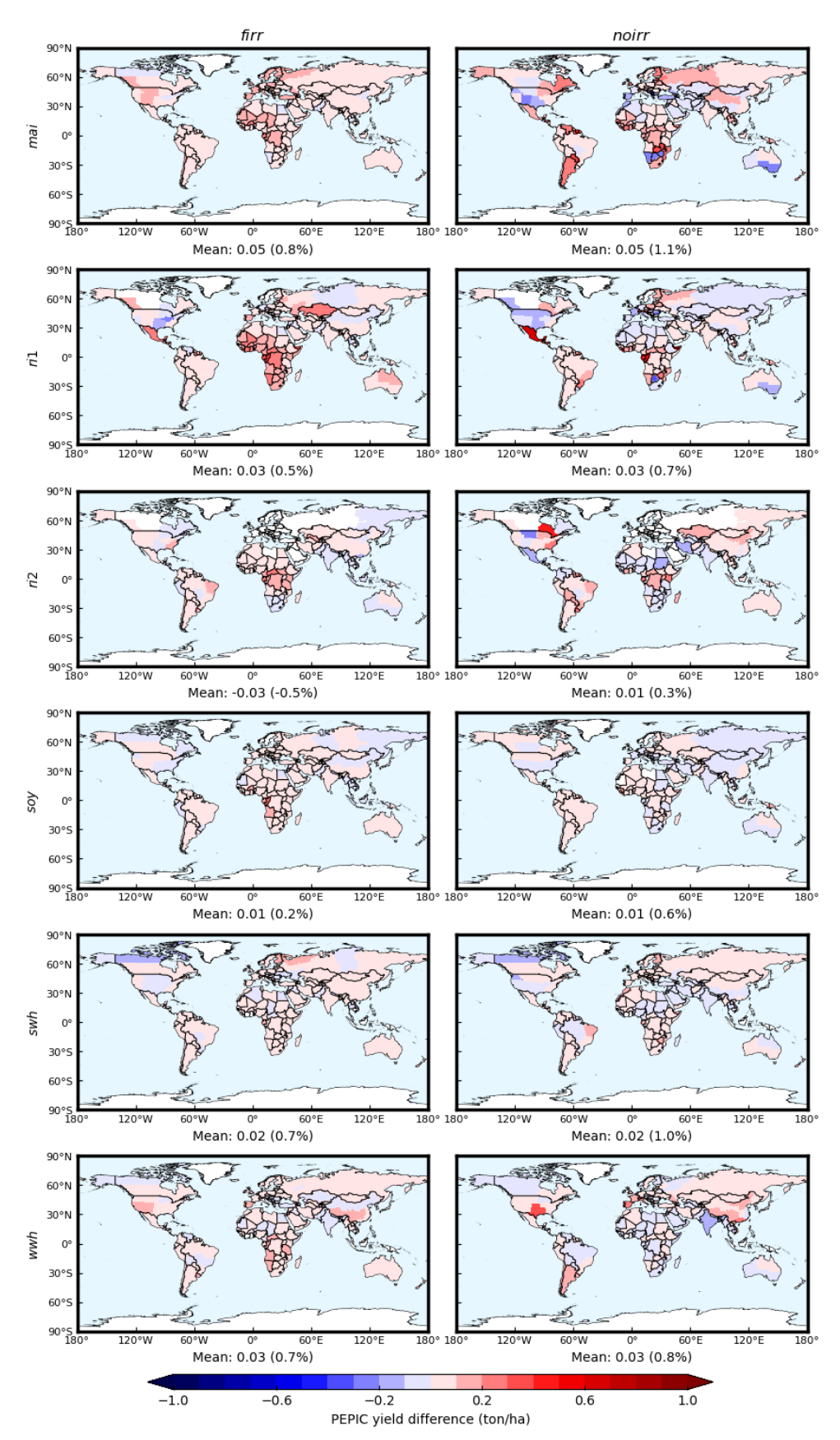


Figure S16. Yield differences between original and PEPIC-based emulated crop yields under SSP585.

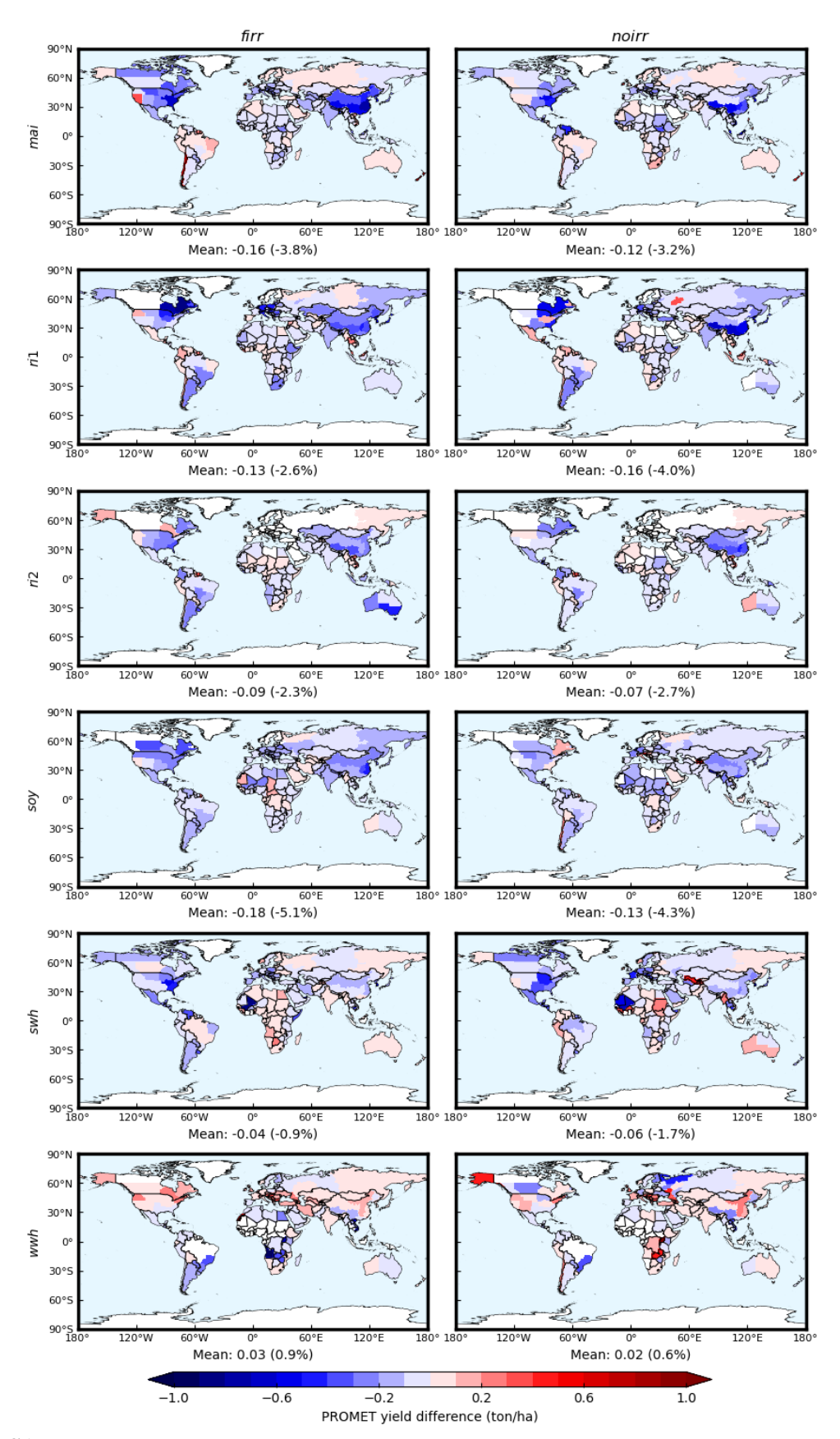


Figure S17. Yield differences between original and PROMET-based emulated crop yields under SSP585.

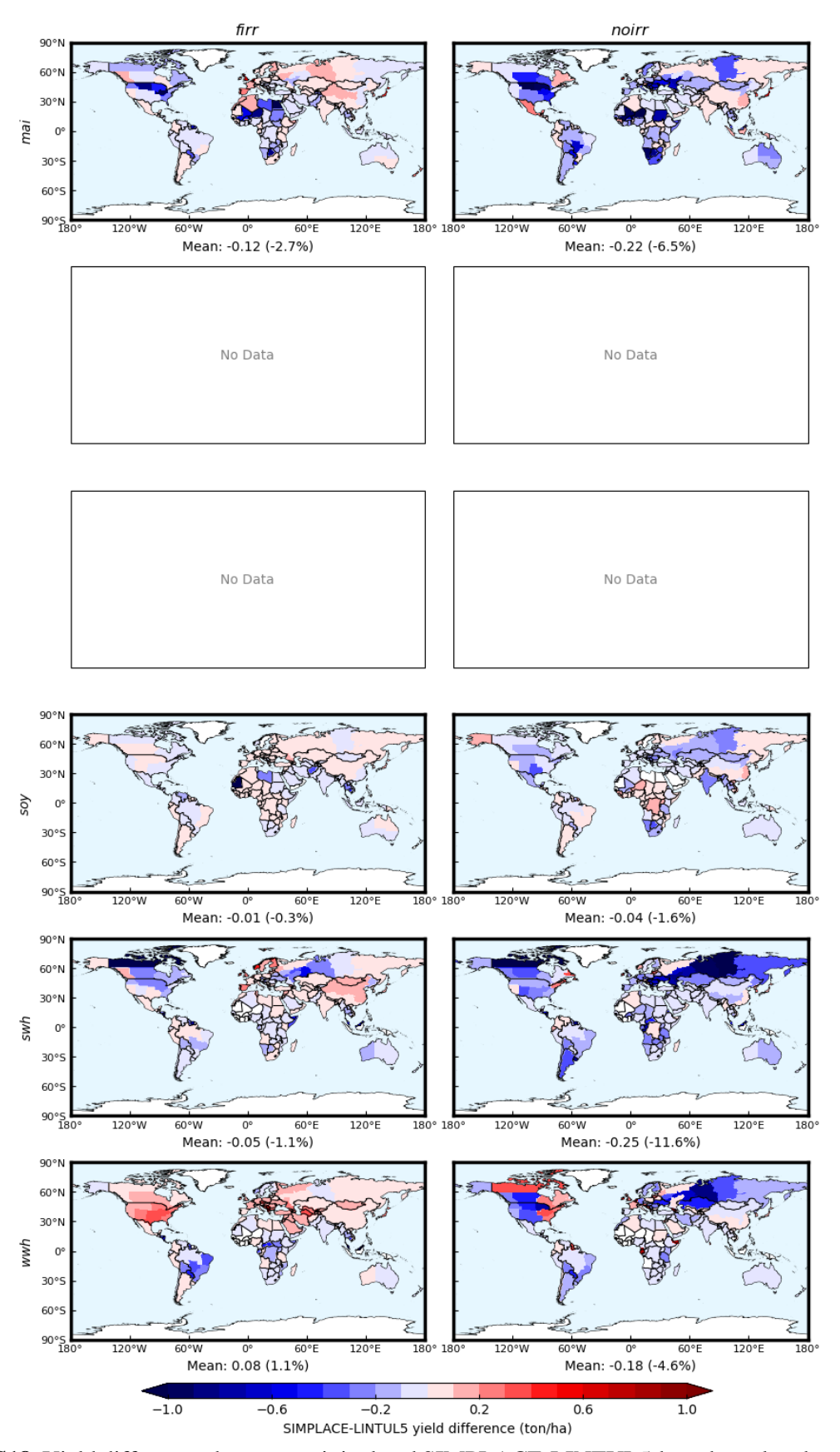


Figure S18. Yield differences between original and SIMPLACE-LINTUL5-based emulated crop yields under SSP585.

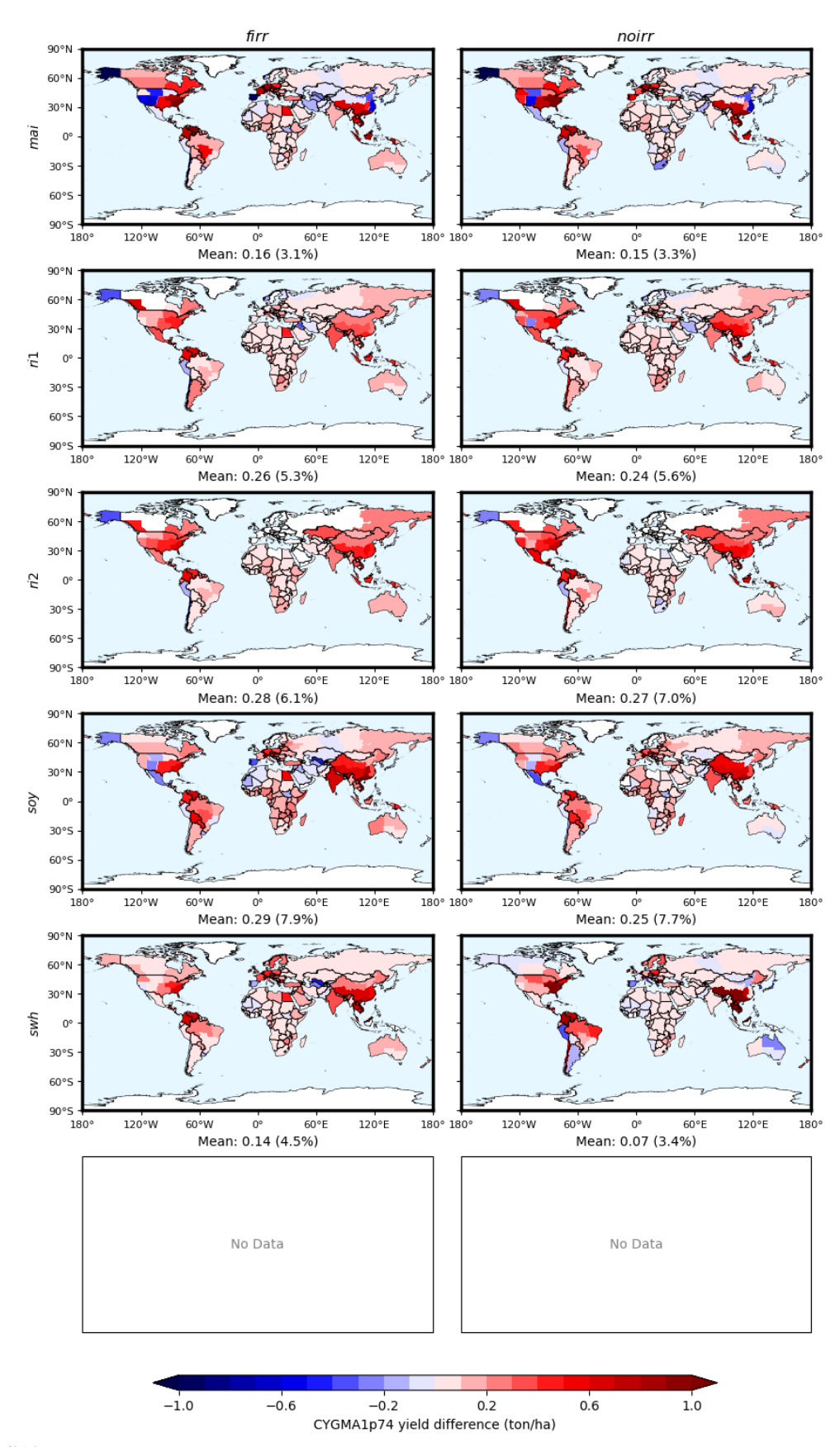


Figure S19. Yield differences between original and CYGMA1p74-based emulated crop yields under GSWP3-W5E5 climate.

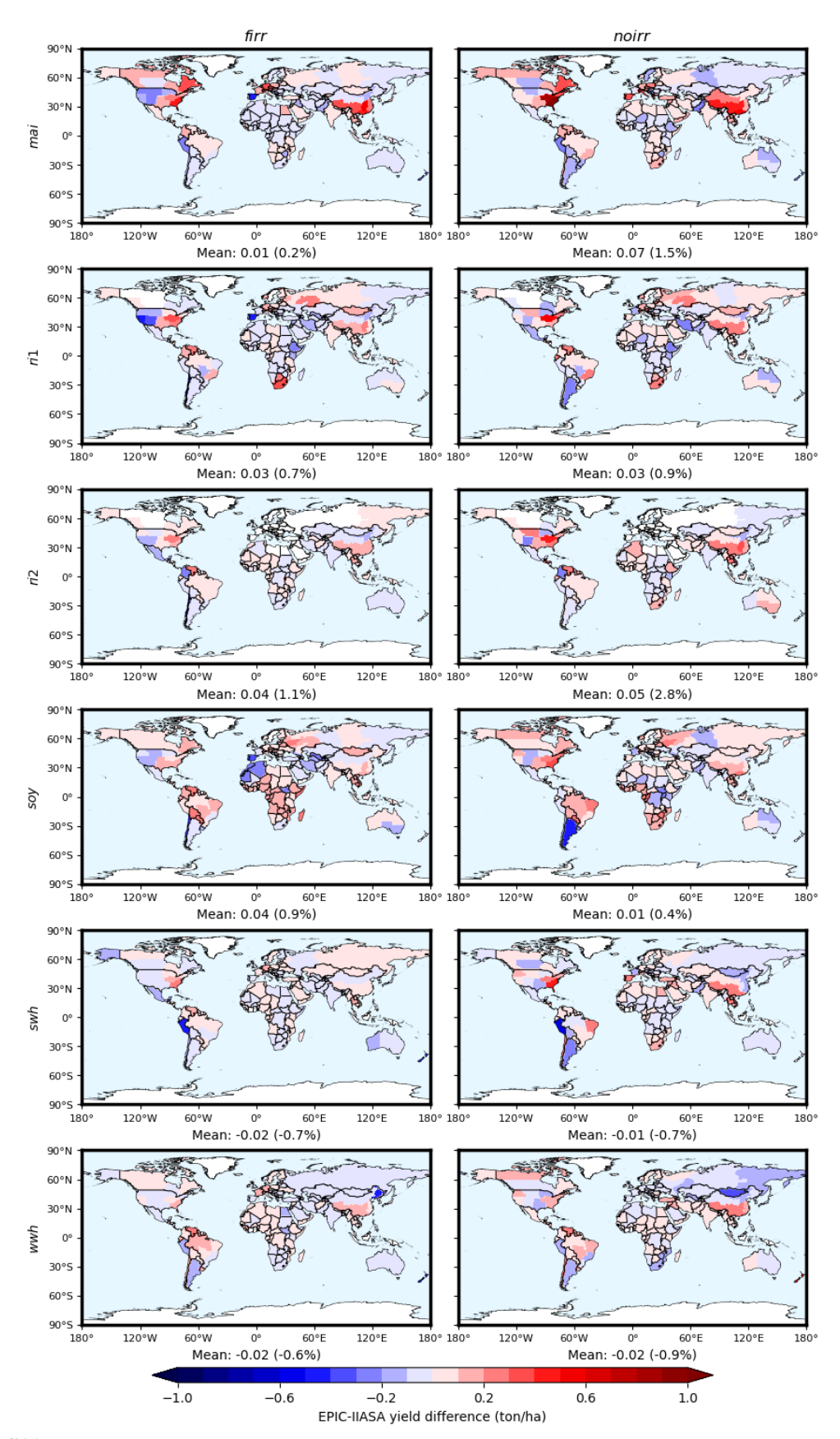


Figure S20. Yield differences between original and EPIC-IIASA-based emulated crop yields under GSWP3-W5E5 climate.

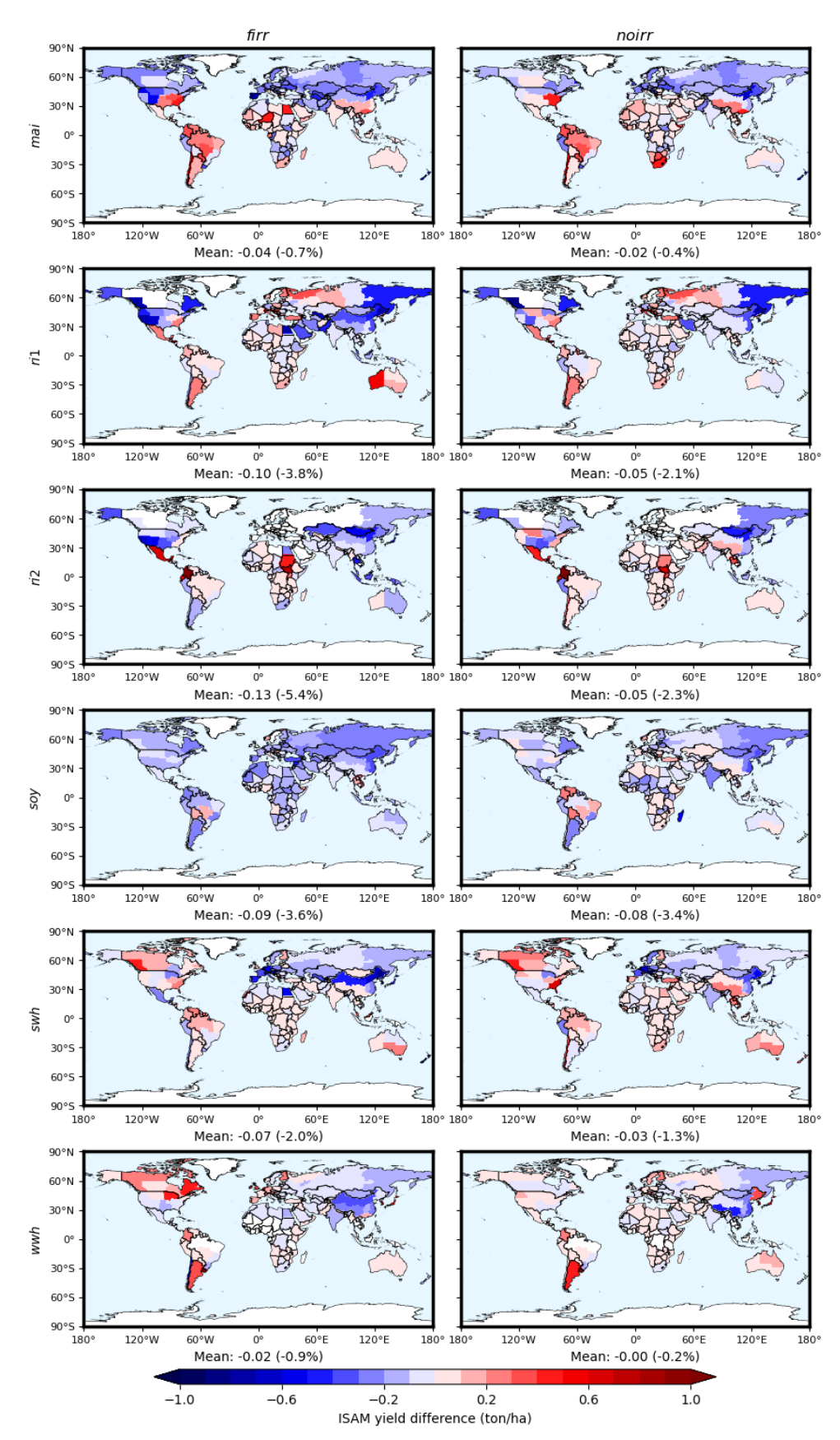


Figure S21. Yield differences between original and ISAM-based emulated crop yields under GSWP3-W5E5 climate.

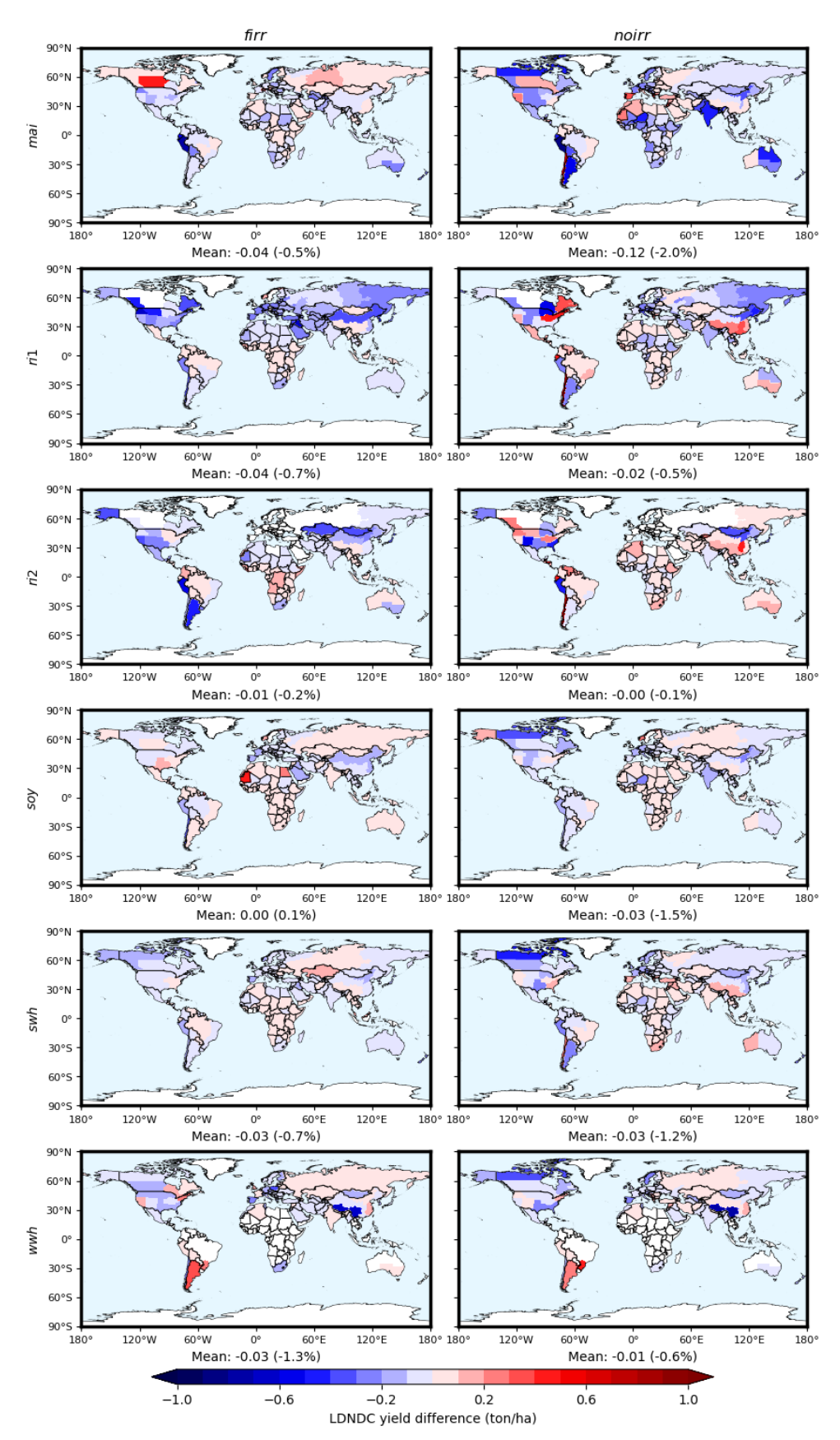


Figure S22. Yield differences between original and LDNDC-based emulated crop yields under GSWP3-W5E5 climate.

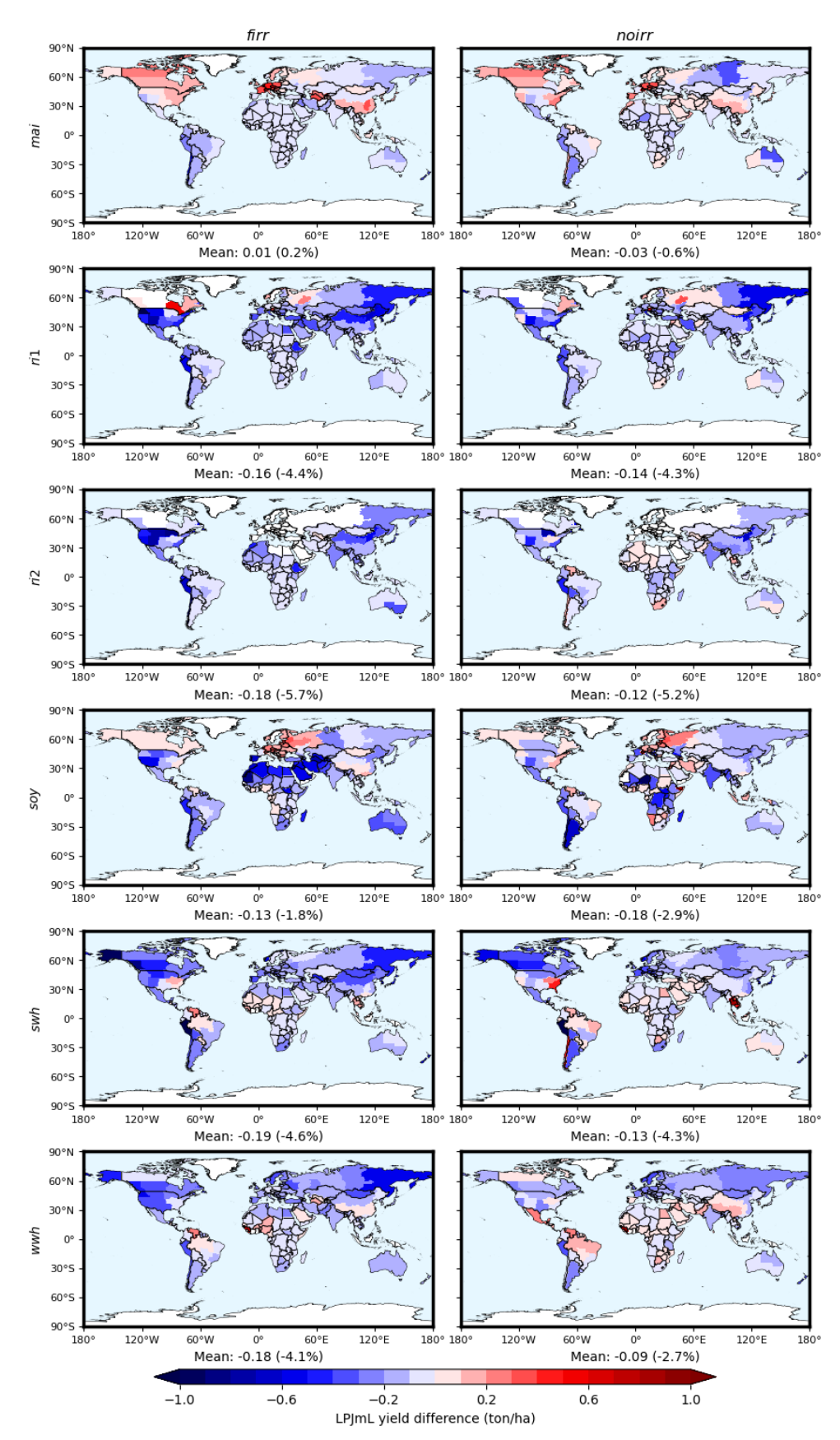


Figure S23. Yield differences between original and LPJmL-based emulated crop yields under GSWP3-W5E5 climate.

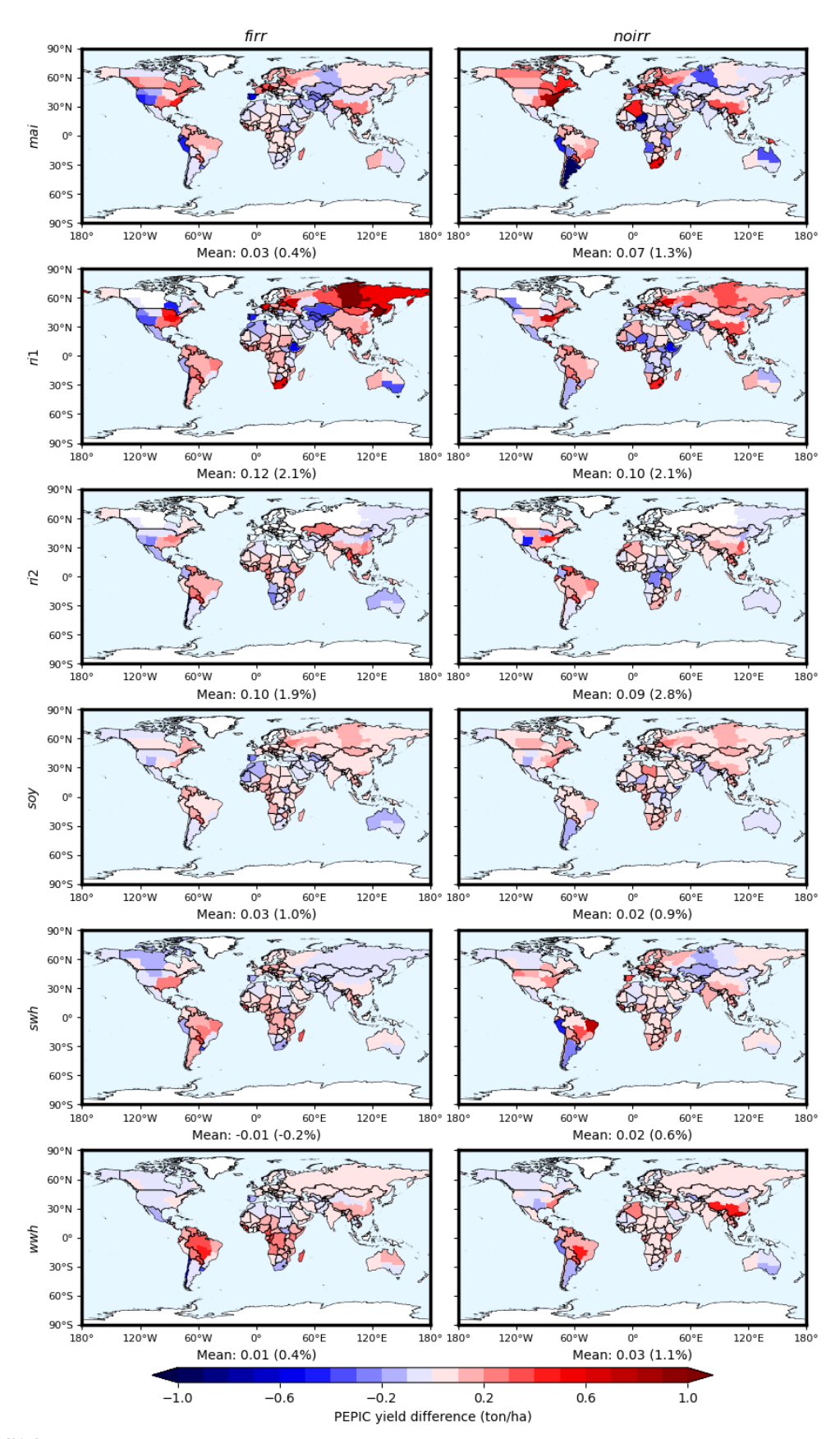


Figure S24. Yield differences between original and PEPIC-based emulated crop yields under GSWP3-W5E5 climate.

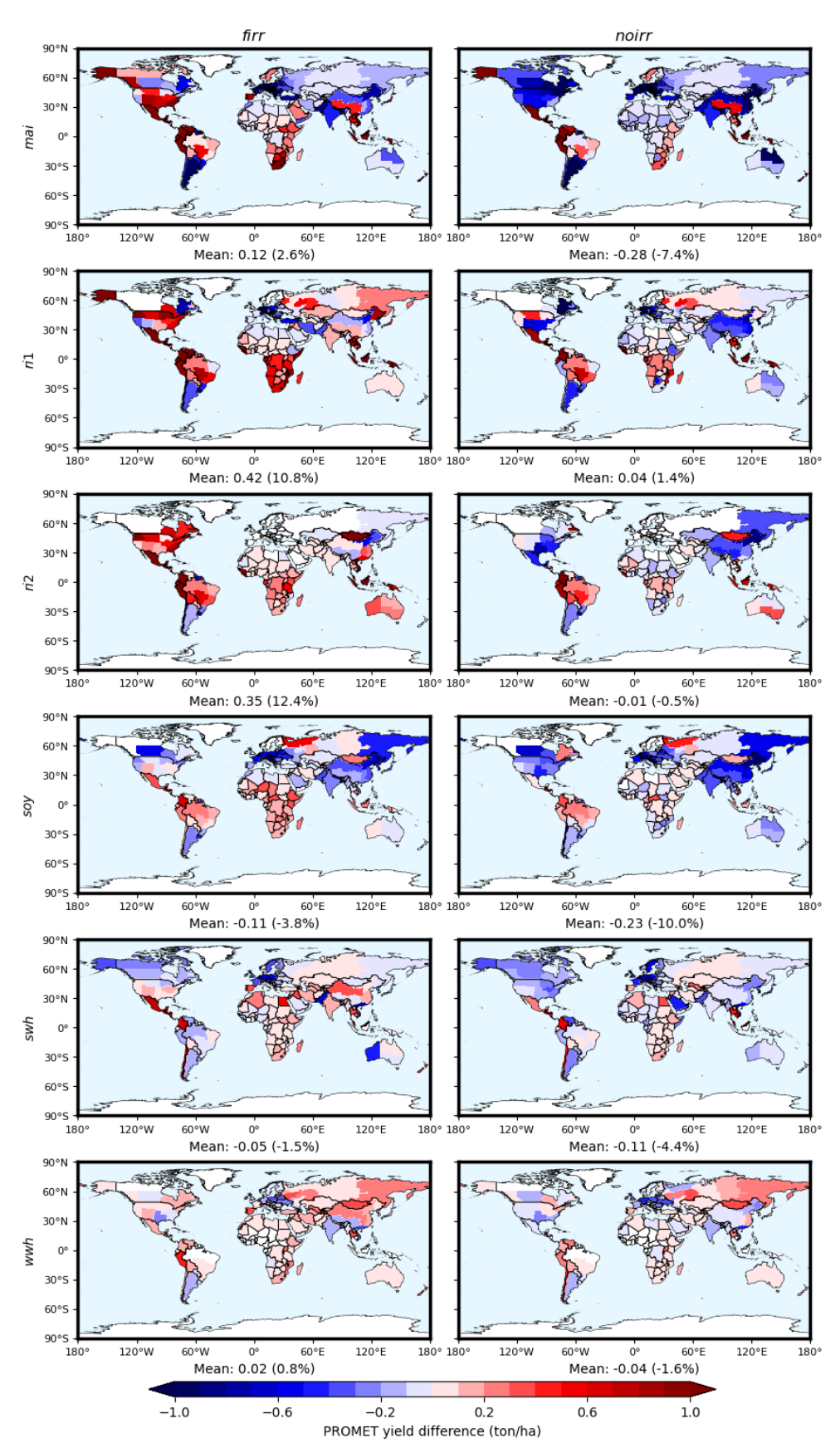


Figure S25. Yield differences between original and PROMET-based emulated crop yields under GSWP3-W5E5 climate.

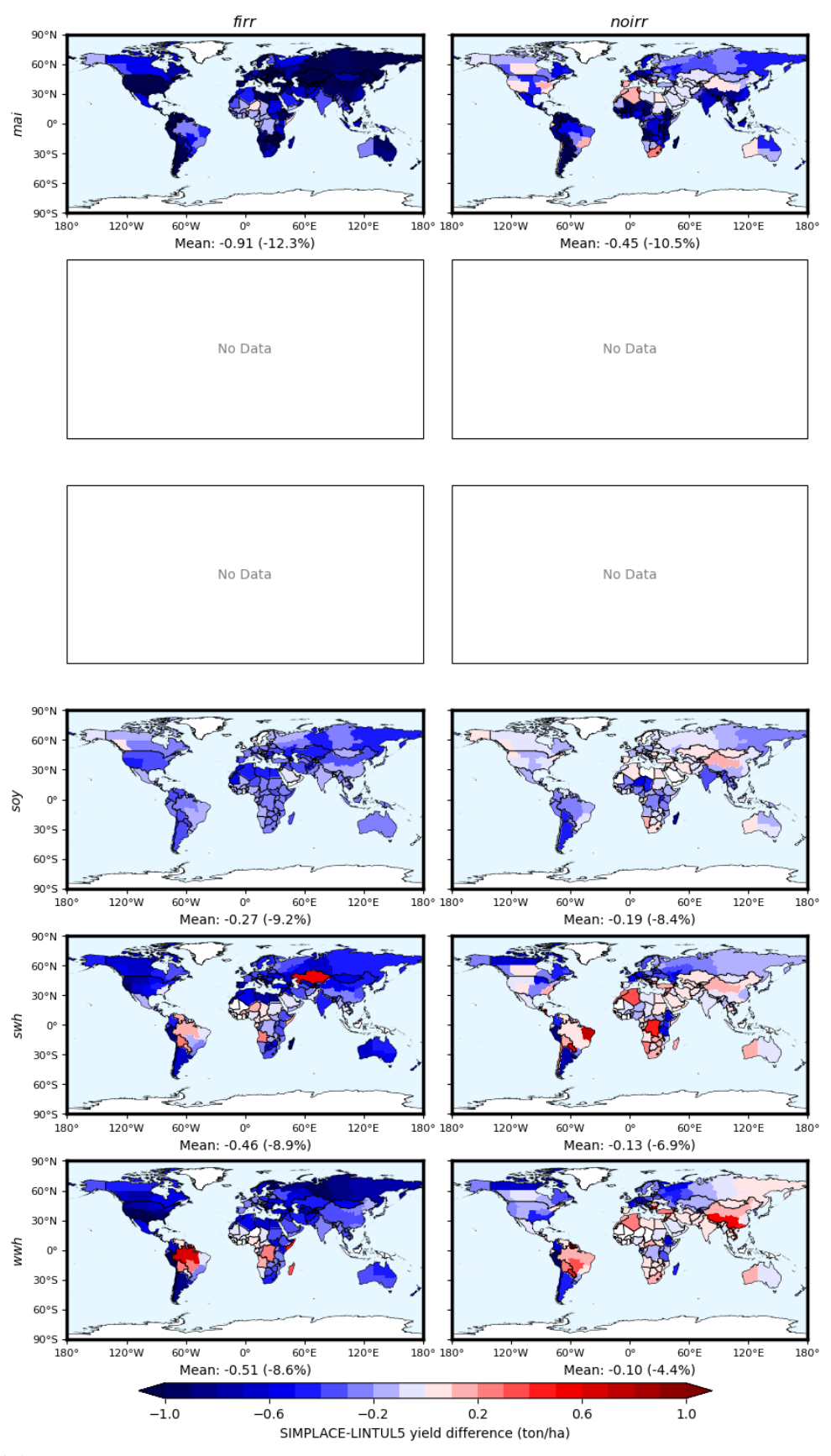


Figure S26. Yield differences between original and SIMPLACE-LINTUL5-based emulated crop yields under GSWP3-W5E5 climate.

 $\textbf{Table S1.} \ \text{Six major production regions by crop.}$

| Cron | Regions | | | | | | |
|---------|----------------|----------------|-----------|----------------|-----------|--------|--|
| Crop | R1 | R2 | R3 | R4 | R5 | R6 | |
| Maize | USA | Mainland China | Brazil | EU27 | Argentina | Others | |
| Rice | Mainland China | India | Indonesia | Bangladesh | Vietnam | Others | |
| Soybean | Brazil | USA | Argentina | Mainland China | India | Others | |
| Wheat | EU27 | Mainland China | India | Russia | USA | Others | |

 Table S2. Crops and corresponding land-use categories.

| Crop Specifier | | Land-use variables | |
|---|---|--|--|
| Maize | Maize mai maize_rainfed, maize_irriga | | |
| Rice (first growing season) | ri1 | rice_rainfed, rice_irrigated | |
| Rice (second growing season) | cond growing season) ri2 rice_rainfed, rice_irrigated | | |
| Soybean soy oil_crops_soybean_rainfed, oil_crops_ | | oil_crops_soybean_rainfed, oil_crops_soybean_irrigated | |
| Spring wheat swh temperate_cereals_rainfed, temperate_cere | | temperate_cereals_rainfed, temperate_cereals_irrigated | |
| Winter wheat wwh temperate_cereals_rainfed, temperate_cerea | | temperate_cereals_rainfed, temperate_cereals_irrigated | |

 $\textbf{Table S3.} \ \textbf{Functional forms and parameters for GGCM-based calibration}.$

| Number | Functional form | Parameters | Descriptions | Maximum point | Asymptotic maximum value |
|--------|---|------------|------------------------|---|--------------------------------|
| 1 | $\alpha x + 1$ | α | Linear | / | / |
| 2 | $e^{\alpha x}$ | α | Exponential | / | / |
| 3 | $e^{(-\alpha\times(x-\beta)^2+\alpha\beta^2)}$ | α, β | Bell-shaped | $x = \beta$ $y = e^{\alpha \beta^2}$ | / |
| 4 | $\frac{2}{e^{ax} + e^{-bx}}$ | α, β | Peak-and- decline | $x = \frac{\ln \beta - \ln \alpha}{\alpha + \beta}$ $y = \frac{2\alpha}{\alpha + \beta} \left(\frac{\beta}{\alpha}\right)^{\frac{\beta}{\alpha + \beta}}$ | / |
| (5) | $\frac{e^{\beta}+1}{e^{-\alpha x+\beta}+1}$ | α, β | S-shaped | | $y = e^{\beta} + 1$ |
| 6 | $\frac{e^{-\alpha\gamma} + e^{\beta\gamma}}{e^{\alpha(x-\gamma)} + e^{-\beta(x-\gamma)}}$ | α, β, γ | Skewed bell- shaped | $x = \gamma + \frac{\ln\beta - \ln\alpha}{\alpha + \beta}$ $y = \frac{\alpha(e^{-\alpha\gamma} + e^{\beta\gamma})}{\alpha + \beta} (\frac{\beta}{\alpha})^{\frac{\beta}{\alpha + \beta}}$ | / |
| 7 | $(\frac{e^{\beta}+1}{e^{-\alpha x+\beta}+1})^{\gamma}$ | α, β, γ | Skewed S- shaped | / | $y = (e^{\beta} + 1)^{\gamma}$ |

Table S4. Parameter limits for each driver and functional form.

| Functional | Parameter | $(CO_2 - CO_{22015})/CO_{22015}$ | | $T_{gs}^c - T_{gs,pi}^c$ | | $(P_{gs}^c - P_{gs,pi}^c)/P_{gs,pi}^c$ | |
|------------|-----------|----------------------------------|-------------|--------------------------|-------------|--|-------------|
| form | | Lower limit | Upper limit | Lower limit | Upper limit | Lower limit | Upper limit |
| 1 | α | -1 | 1 | -10 | 10 | -1000 | 1000 |
| 2 | α | -10 | 10 | -10 | 10 | -10 | 10 |
| | α | 0 | 10 | 0 | 10 | 0 | 10 |
| 3 | β | -1 | 4 | -30 | 30 | -1 | 100 |
| | α | 0 | 10 | 0 | 10 | 1 | 10 |
| 4 | β | 0 | 10 | 0 | 10 | 0 | 10 |
| | α | 0 | 100 | 0 | 100 | 0 | 100 |
| 5 | β | -10 | 10 | -10 | 10 | -10 | 10 |
| 6 | α | 0 | 100 | 0 | 100 | 0 | 100 |
| | β | 0 | 100 | 0 | 100 | 0 | 100 |
| | γ | -10 | 10 | -10 | 10 | -10 | 10 |
| T | α | 0 | 100 | 0 | 100 | 0 | 100 |
| | β | -10 | 10 | -10 | 10 | -10 | 10 |
| | γ | 0 | 10 | 0 | 10 | 0 | 10 |

Table S5. GGCM-irrigation-crop combinations of extreme-value yield responses with corresponding regional occurrences.

| GGCM | Irrigation | Crop (Occurrence) | |
|------------------------|------------|---|--|
| CYGMA1p74 | noirr | mai (9), ri1 (8), ri2 (5), soy (7), swh (34) | |
| LDNDC noirr | | mai (9) | |
| I DI I | firr | ri1 (4), ri2 (1) | |
| LPJmL | noirr | mai (4), ri1 (18), ri2 (17), soy (14), swh (6), wwh (7) | |
| PEPIC | noirr | mai (1) | |
| PROMET noirr | | mai (6), ri1 (9), ri2 (7), soy (8), swh (3), wwh (2) | |
| SIMPLACE-LINTUL5 noirr | | soy (2), wwh (1) | |

Extreme-value yield occurrences are in parentheses.

 $\textbf{Table S6.} \ \textbf{Functional forms and parameters for nitrogen responses.}$

| Model | Functional form | Parameters |
|------------------|--------------------------------|------------|
| Michaelis-Menten | $\frac{\alpha x}{x+\beta}$ | α, β |
| Mitscherlich | $\alpha(e^{\beta x}-1)$ | α, β |
| George | $\alpha(0.99^x - 1) + \beta x$ | α, β |